Supplement to Intercomparison of airborne and surface-based measurements during the CLARIFY, ORACLES and LASIC field experiments

Intercomparison of airborne and surface-based measurements during the CLARIFY, ORACLES and LASIC field experiments

Paul A. Barrett[1], Steven J. Abel[1], Hugh Coe[2], Ian Crawford[2], Amie Dobracki[3,], James Haywood[4,1], Steve Howell[5], Anthony Jones[1,4], Justin Langridge[1], Greg M. McFarquhar[6,7], Graeme J. Nott[8], Hannah Price[8], Jens Redemann[6], Yohei Shinozuka[9], Kate Szpek[1], Jonathan W. Taylor[2], Robert Wood[10], Huihui Wu[2], Paquita Zuidema[3], Stéphane Bauguitte[8], Ryan Bennett[11], Keith Bower[2], Hong Chen[12], Sabrina Cochrane[12], Michael Cotterell[4,13], Nicholas Davies[4,14], David Delene[15], Connor Flynn[16], Andrew Freedman[17], Steffen Freitag[5], Siddhant Gupta[6,7], David Noone[18,19], Timothy B. Onasch[17], James Podolske[20], Michael R. Poellot[15], Sebastian Schmidt[12,21], Stephen Springston[22], Arthur J. Sedlacek III[22], Jamie Trembath[8], Alan Vance[1], Maria Zawadowicz[22], Jianhao Zhang[3,23,24]

[1]Met Office, Exeter, EX1 3PB, UK
[2]Department of Earth and Environmental Sciences, University of Manchester, M13 9PL, UK
[3]Rosential School of Marine and Atmospheric Science, University of Miami, Miami, FL 33149, USA
[4]University of Exeter, Exeter, EX4 4PY, UK
[5]Department of Oceanography, University of Hawai'i at Mānoa,, Honolulu, HI, USA
[6]School of Meteorology, University of Oklahoma, Norman, OK, USA
[7]Cooperative Institute for Severe and High-Impact Weather Research and Operations, University of Oklahoma, Norman, OK, USA
[8]FAAM Airborne Laboratory, Cranfield, MK43 0AL, UK
[9]Universities Space Research Association, Columbia, MD, USA
[10]Department of Atmospheric Sciences, University of Washington, Seattle, WA, USA
[11]Bay Area Environmental Research Institute, NASA Ames Research Centre, Moffett Field, Mountain View, CA, USA
[12]Department of Atmospheric and Oceanic Sciences, University of Colorado, Boulder, CO, USA
[13]School of Chemistry, University of Bristol, Bristol, BS8 1TS, UK
[14]Haseltine Lake Kempner, Bristol, BS1 6HU, UK
[15]Department of Atmospheric Sciences, University of North Dakota, Grand Forks, ND, USA
[16]School of Meteorology, University of Oklahoma, Norman, OK, USA
[17]Aerodyne Research Inc., Billerica, MA, USA
[18]College of Earth, Ocean, and Atmospheric Sciences, Oregon State University, Corvallis OR, USA
[19]Department of Physics, University of Auckland, Auckland, New Zealand
[20]NASA Ames Research Centre, Moffett Field, Mountain View, CA, USA
[21]Laboratory for Atmospheric and Space Physics, University of Colorado, Boulder, CO, USA
[22]Brookhaven National Laboratory, Upton, NY, USA
[23]NOAA Chemical Sciences Laboratory (CSL), Boulder, CO, USA
[24]Cooperative Institute for Research in Environmental Sciences (CIRES) at the University of Colorado Boulder, Boulder, CO, USA

Correspondence to: Paul A. Barrett (paul.barrett@metoffice.com)

1 FAAM atmospheric radiation calibration procedures

The Eppley pyranometers were calibrated against laboratory standards on the ground at Cranfield, UK before the deployment. Before each flight, the Eppley pyranometers were accessed and cleaned to remove any build-up of dirt from aerosols impacted on the leading face of the instrument. Lower BBRs do not require pitch and roll corrections owing to the upwelling radiation being diffuse. Upper BBR calibration procedures typically involve 'box-patterns' where the aircraft flies 4 sequential orthogonal legs at a constant high altitude. High altitude is chosen so that the atmospheric radiation measurements are free from the influence of any cloud and water vapour variations above the aircraft. This results in four sets of measured irradiances at headings of approximately 90° to one another and standard pitch and roll correction algorithms that account for changes in the solar zenith angle (Jones et al., 2018) are applied in order to effectively minimise the variation between these four sets of observations.

In addition to box-patterns, during CLARIFY-2017 the aircraft performed a series of "pirouettes" before take-off and after landing which consisted simply of turning the aircraft through 360° while the aircraft was on the runway and measuring the broad-band irradiance as a function of the relative solar heading. Ideally these pirouettes should be performed in cloud- and aerosol-free conditions, as far as practicable, both before and after a sortie. In practice, there was isolated cumulus and broken stratocumulus cloud over the Wideawake airfield at Ascension Island. As per almucantar scans performed by AERONET (Dubovik et al., 2000), the presence of clouds can significantly interfere with the measurements. Nevertheless, if used judiciously, pirouette manoeuvres offer some significant advantages over box-patterns; they are quick, they do not eat into airborne science time and they provide effectively continuous data at all angles relative to the sun rather than just four headings.

SHIMS calibration for CLARIFY-2017 was based on laboratory measurements using a traceable standard lamp, and a field transfer standard. However, repeated laboratory calibrations have previously shown differences of up to 7 % (Vance et al. 2017). The calibration procedure failed to produce acceptable results when compared to radiative transfer calculations of the spectral flux, with a constant, but unexplained offset of around a factor of 1.30 ± 0.06 (2s) as a campaign mean for both upper and lower SHIMS instruments (see Jones et al., 2018 for full details). In contrast, when irradiances from the clear-domed BBRs are compared to radiative transfer calculations accounting for the extended wavelength range of these instruments (Jones et al., 2018) they are found to be within the instrumental error of the BBRs of 3 % (Hignett et al., 1999). Therefore, a single campaign mean correction of 1.3 was applied to the SHIMS measurements based on the BBR data and idealised radiative transfer simulations (Edwards and Slingo, 1996). Note that difficulties in accurately determining absolute calibrations from standard lamps necessitating additional correction procedures has been highlighted before (e.g., Schmid et al., 1998). While this procedure is not ideal and leads to uncertainties in the absolute irradiance of around 5 % (at 95 % confidence), the opportunity of performing an intercomparison flight with the NASA P3 aircraft allowed it to be tested.

As with the BBR instruments, the SHIMS instrument is canted 3° forward relative to the airframe. Analysis of box-patterns and pirouettes are performed in an analogous manner to that for the BBRs. Jones et al. (2018) have documented the pitch and roll corrections for CLARIFY-2017 in detail with Fig. S1 showing a summary of those results from two box patterns and two pirouettes for the clear 0.3-3.0 μm BBR and the 0.30–0.95 μm SHIMS module. The pitch and roll corrections, applied uniformly to measurements across the CLARIFY-2017 campaign, for the BBR instrument are -3.2° and 0° respectively and for the SHIMS instrument are -3.0° and +0.3° respectively. In both the box patterns and the pirouettes performed after flights, evidence was seen of a so called 'dirty-dip' in which the front face of the BBR and SHIMS instruments had sufficient aerosol impacted upon them to reduce the transmission of the radiometer dome. Our protocol is therefore to exclude data that might be affected by any dirty-dip, i.e., excluding any irradiance data inside of ±40°. We also apply this criterion to estimate the potential error owing to pitch and roll corrections.

The utility of the pirouettes was noted when performing pitch and roll corrections (Jones et al., 2018). In particular, the pirouette method for calibrating the pitch and roll offsets of the BBR and SHIMS upper appears to reduce the uncertainties owing to pitch and roll corrections by around a factor of two when compared to the box patterns to less than 1 % (95 % confidence interval) but is susceptible to errors and uncertainties caused by cloud. The ease of making these measurements and the reductions in uncertainties, means that, providing there are opportunities for making measurements in cloud-free conditions, pirouette manoeuvres should be performed for all sorties focussing on broadband and spectral radiative measurements on the FAAM aircraft. Note that the uncertainties that are presented here refer only to the corrections to pitch and roll. The total uncertainty in the SHIMS measurements is difficult to establish owing to the failure of the absolute

calibration procedure when the SHIMS instrument is installed on the aircraft. An approximate uncertainty estimate may be obtained by root mean squared analysis based on the variability in the correction factor to the BBR data (±5 %), the estimated error in the BBRs themselves (±3 %), the pitch and roll corrections (±1 %) and the differences in the azimuthal sensitivity of the SHIMS and BBR data (±1 %), yielding at least 6 % uncertainty. Thus, the intercomparison flight provides an extremely important opportunity to assess the consistency of the data against that from the NASA P3 instrumentation.

2 NASA P3 PSAP absorption correction

Corrections to the absorption coefficient (σ_{AP}) data that were applied in real-time by the P3 PSAP firmware during the 2017 ORACLES campaign were first removed prior to re-processing with the Virkkula (2010) correction method. Following Pistone et al. (2019, App. A1), both wavelength-specific and wavelength-averaged corrections to the σ_{AP} data were tested in this study. Based on data from ORACLES-2016 only, Pistone et al. (2019) showed that the calculated wavelength dependence of absorption is stronger for the wavelength-specific corrections. However, this results in a reduction in the derived ω_0 the between the 470 and 530 nm wavelengths which is counter-intuitive based on previous work (e.g., as summarised by Wu et al. 2020). The results from the runBL boundary layer sampling leg, behind the PM1 impactor, exhibited similar behaviour to that shown by Pistone et al. (2019) . As such, this study only uses data from the wavelength-averaged correction method and maintains consistency with the LASIC dataset.

Some 25 % of the optical scattering observed during the boundary layer sampling leg runBL was due to aerosol particles, likely to be sea-salt, larger than 1.0 μm (Fig. 5 (f), (g), Fig. 6). Since aerosol scattering data is required in order to correct the PSAP data, this will add uncertainty to the Virkkula (2010) corrected PSAP σ_{AP} data when only the nephelometer was sampling behind the PM1 impactor.

3 FAAM BAe-146 CDP bin dimensions calibration

A 10-point glass beads calibration of the FAAM CDP was performed before each day of flying throughout the CLARIFY campaign with beads of known, traceable, mean diameter and standard deviation. The calibration beads were dispensed into a specially made dispensing vial and gently blown into the instrument sample volume using a can of compressed air. The exit tube of the dispenser locates into a calibration jig which clamps onto the instrument to deliver the particles into the sample area. Comprehensive details of the method can be found in the CDP manual (DMT DOC-0343, Rev A).

For each bead calibration the modal bin diameter mid-point (as provided by FAAM) was chosen as the instrument sizing response, using the CDP default bins (DMT DOC-0343, Rev A). This nominal diameter was then compared to the water corrected size of the bead using $D_{Corr} = 0.8 * D_{bead}+0$, thus producing a 10-point linear scatter of the instrument response for each diameter. A fit to the 10-point calibration was found using a 2000 iteration Monte Carlo simulation (MATLAB custom linfitxy function) where the water corrected standard deviation for each bead is used as the input to the error in the bead size and the modal bin width divided by two is used as the input to the error in the instrument sizing response. The modal bin calibration throughout the CLARIFY campaign was found to be reasonably consistent with the variation between calibrations likely to be due to variations in individual calibrations (e.g., difficult conditions to perform a steady calibration) rather than due to significant variation in instrument response.

The linear fit applied to the campaign median calibration response using the method outlined above was found to be Y = (1.074 ± 0.034) * X + (-0.22 ±0.57), which results in a maximum of 7 % change to bin dimensions. The resulting bin centres and widths from this fit are used in subsequent analysis (Table S1). Comparisons were made between the integrated LWC from observed CDP PSDs with those from the Nevzorov 2 mm diameter LWC sensor which is less sensitive to larger droplets than the 3 mm sensor (e.g., Strapp et al., 2003). It was found that this simple linear fit provided a good overall comparison to the Nevzorov Liquid Water Content (LWC) and adiabatic LWC profiles over a wide range of modal cloud droplet sizes as can be seen from Fig. S2, certainly for effective diameters (ED) below 35 μm. At larger sizes the comparison is somewhat weaker, but also less robust, due to reducing collection efficiency of the Nevzorov 2 mm LWC sensor at larger particle sizes.

4 Aerosol mass spectrometers

The CLARIFY data (Wu et al. 2020) showed that sulphate was fully neutralised in both the boundary layer and free troposphere (Fig. S3). However, the ORACLES data suggested less neutralised sulphate (Dobracki et al. 2021). To aid understanding of these differences, the ORACLES AMS data was analysed using both the PIKA (the Particle Integration by Key v.1.16 algorithm) and SQUIRREL (SeQUential Igor data RetRiEval) algorithms. Data from the non-HR AMS deployed by the UK CLARIFY campaign can only be analysed using the SQUIRREL software. The comparison assessed the contribution of differences between the SQUIRREL/PIKA fragmentation tables to differences in the reported sulphate mass concentrations. When analysed using the SQUIRREL algorithm, the ORACLES AMS estimate of the sulphate mass concentration was lower than that calculated when using PIKA by approximately 7 %. This indicates that the ORACLES and CLARIFY AMS-derived aerosol mass concentrations can be meaningfully compared, with the CLARIFY campaign sampling fully neutralized nitrate aerosol, and the ORACLES campaign in 2016 sampling aerosol for which the formation of inorganic nitrate was mildly suppressed, based on (Zhang et al., 2007).

5. NASA P3 and FAAM BAe146 SP2 data

As noted in the main text a leak was identified which affected the NASA P3 airborne data at times immediately prior to, and likely during, the airborne intercomparisons. here we reproduce the observation for completeness (Table. S2) although these do not represent the state of the comparisons that would be expected should both systems be performing optimally. The leak itself was spotted rapidly during the NASA P3 flight and dealt with for subsequent flights.

References

Dubovik, O., Smirnov, A., Holben, B. N., King, M., Kaufman, Y. J., Eck, T. F., and Slutsker, I.: Accuracy assessment of aerosol optical properties retrieval from AERONET Sun and sky radiance measurements, J. Geophys. Res., 105, 9791–9806, 2000.

DMT: Cloud Droplet Probe (CDP-2) Operator Manual DOC-0343, Rev A, https://www.dropletmeasurement.com/product/cloud-droplet-probe/, Last_accessed: 11 November 2021.

Dobracki, A., Howell, S., Saide, P., Freitag, S., Aiken, A. C., Burton, S., Coe, H., Sedlacek III, A. J., Taylor, J., Wu, H., Redemann, J., Wood, R., and Zuidema, P.: Non-reversible aging increases the solar absorptivity of African biomass burning plumes, Earth and Space Science Open Archive, https://doi.org/10.1002/essoar.10507561.1, https://www.essoar.org/doi/abs/10.1002/essoar.10507561.1, 2021.

Edwards, J. M. and Slingo, A.: Studies with a flexible new radiation code. I: Choosing a configuration for a large-scale model. Quarterly Journal of the Royal Meteorological Society, 122(531), 689-719, 1996.

Hignett, P., Taylor, J. P., Francis, P. N., and Glew, M. D.: Comparison of observed and modeled direct aerosol forcing during TARFOX. Journal of Geophysical Research: Atmospheres, 104(D2), 2279-2287, 1999.

Jones, A. C., Haywood, J. M., Vance, A., and Ryder, C.: Pitch and roll corrections for the CLARIFY-2017 radiation data, Met Office, OBR Technical Note 91, https://library.metoffice.gov.uk/Portal/Default/en-GB/RecordView/Index/646187, © Crown Copyright 2018. Information provided by the National Meteorological Library and Archive – Met Office, UK

Pistone, K., Redemann, J., Doherty, S., Zuidema, P., Burton, S., Cairns, B., Cochrane, S., Ferrare, R., Flynn, C., Freitag, S., Howell, S. G., Kacenelenbogen, M., LeBlanc, S., Liu, X., Schmidt, K. S., Sedlacek III, A. J., Segal-Rozenhaimer, M., Shinozuka, Y., Stamnes, S., van Diedenhoven, B., Van Harten, G., and Xu, F.: Intercomparison of biomass burning aerosol optical properties from in situ and remote-sensing instruments in ORACLES-2016, Atmos. Chem. Phys., 19, 9181–9208, https://doi.org/10.5194/acp-19-9181-2019, 2019.

Schmid, B., Spyak, P. R., Biggar, S. F., Wehrli, C., Sekler, J., Ingold, T., Mätzler, C., and Kämplr, N.: Evaluation of the applicability of solar and lamp radiometric calibrations of a precision Sun photometer operating between 300 and 1025 nm, App. Opt., 37, 18, 3923-3941, 1998.

Strapp, J. W., Oldenburg, J., Ide, R., Lilie, L., Bacic, S., Vukovic, Z., Oleskiw, M., Miller, D., Emery, E., Leone, G.: Wind Tunnel Measurements of the Response of Hot-Wire Liquid Water Content Instruments to Large Droplets, J Atmos. Sci., 20, 6: 791–806, https://doi.org/10.1175/1520-0426(2003)020<0791:WTMOTR>2.0.CO;2, 2003.

Virkkula, A.: Correction of the Calibration of the 3wavelength Particle Soot Absorption Photometer (3λ PSAP), Aerosol Sci. Technol., 44:8, 706–712, https://doi.org/10.1080/02786826.2010.482110, 2010.

Wu, H., Taylor, J. W., Szpek, K., Langridge, J., Williams, P. I., Flynn, M., Allan, J. D., Abel, S. J., Pitt, J., Cotterell, M. I., Fox, C., Davies, N. W., Haywood, J., and Coe, H.: Vertical and temporal variability of the properties of transported biomass burning aerosol over the southeast Atlantic during CLARIFY-2017, Atmos. Chem. Phys., 20, 12697–12719, https://doi.org/10.5194/acp-20-12697-2020 , 2020.

Zhang, Q., Jimenez, J. L., Worsnop, D. R., and Canagarantam, M.: A Case Study of Urban Particle Acidity and Its Influence on Secondary Organic Aerosol. Environ Sci Technol., 41, 3213-3219, doi:10.1021/es061812j, 2007.

Tables and Figures

	BAe146, P3 nominal	BAe146 calibrated
Bin #	Diameter [µm]	Diameter [µm]
1	2	1.9
2	3.5	3.5
3	4.5	4.6
4	5.5	5.7
5	6.5	6.8
6	7.5	7.8
7	8.5	8.9
8	9.5	10.0
9	10.5	11.0
10	11.5	12.1
11	12.5	13.2
12	13.5	14.3
13	15	15.9
14	17	18.0
15	19	20.2
16	21	22.3
17	23	24.4
18	25	26.6

19	27	28.7
20	29	30.9
21	31	33.0
22	33	35.2
23	35	37.3
24	37	39.5
25	39	41.6
26	41	43.7
27	43	45.9
28	45	48.0
29	47	50.2
30	49	52.3

Table S1 Nominal CDP bin centres for FAAM BAe146 and P3 and calibrated bin centres for FAAM BAe-146

Parameter	**Run**	**NASA P3**	**FAAM BAe-146**
Chemical composition			
rBC_n [cm^{-3}]			
Part 1	runBL	81 ± 6	140 ± 11
Part 2	runBL	61 ± 2	121 ± 3
		Y = 0.54x	**Linear regression**
rBC_m [ng m^{-3}]			
Part 1	runBL	225 ± 25	387 ± 29
Part 2	runBL	165 ± 8	340 ± 22
		y = 0.54x	**Linear regression**

Table S2 Summary of comparisons from NASA, FAAM observations of black carbon number (rBC_n) and mass (rBC_m) presented as mean and standard deviations. The linear fit was performed with a fixed intercept of zero.

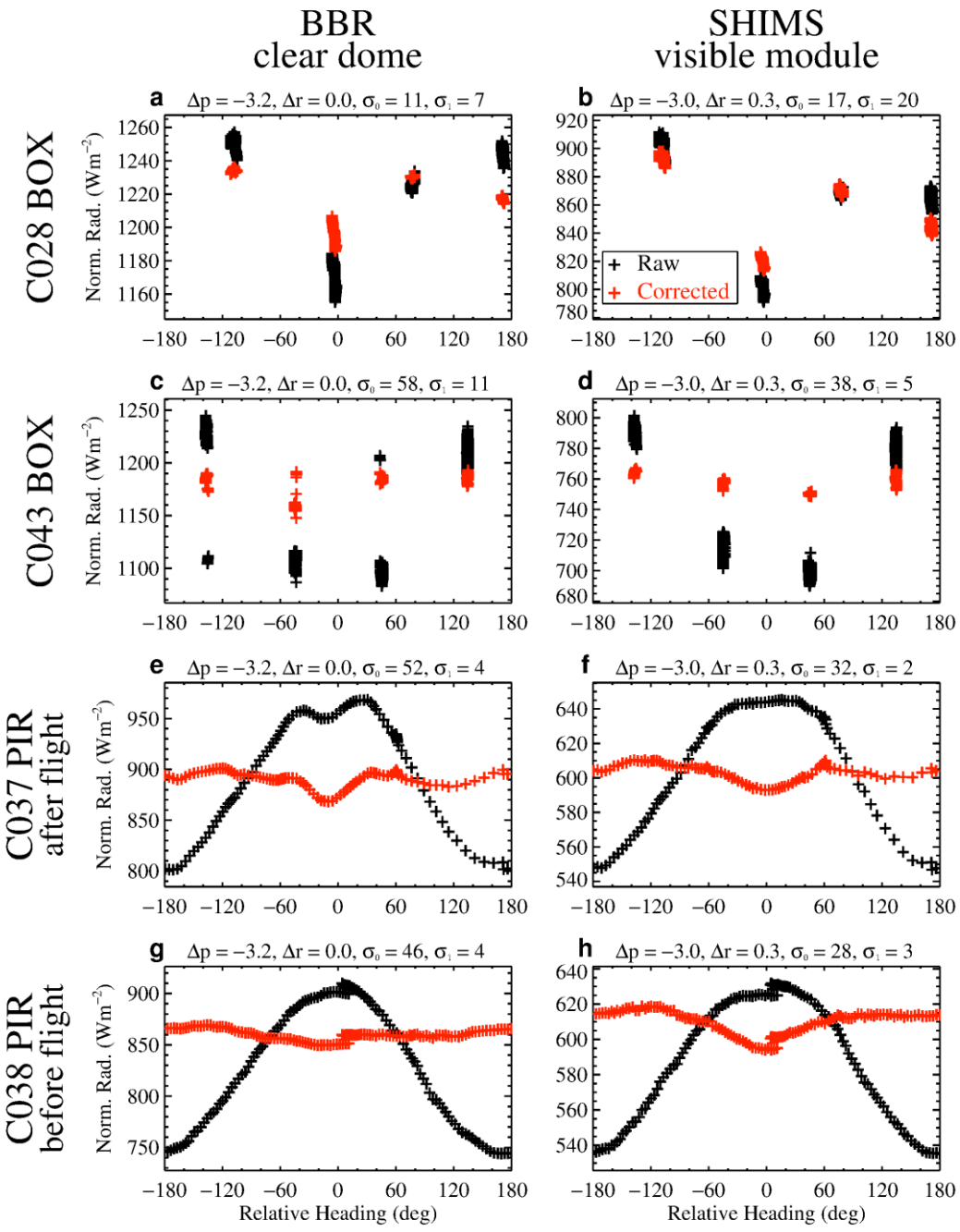

Figure S1 Downwelling shortwave radiation measurements normalized by the cosine of the solar zenith angle from (left) the clear-dome BBR (0.3-3μm) and (right) the SHIMS visible module (0.3-0.95μm). Black crosses indicate raw data and red crosses indicate pitch-and-roll corrected data. Standard deviations for relative headings outside of ±40° are given for the raw data (σ_0) and the corrected data (σ_1) along with pitch (Δp) and roll (Δr) coefficients. Figures (a)-(d) show two high-altitude 4-legged-box manoeuvres, while Figures (e)-(h) show two surface-based aircraft pirouette manoeuvres. Figures reproduced from Jones et al. (2018).

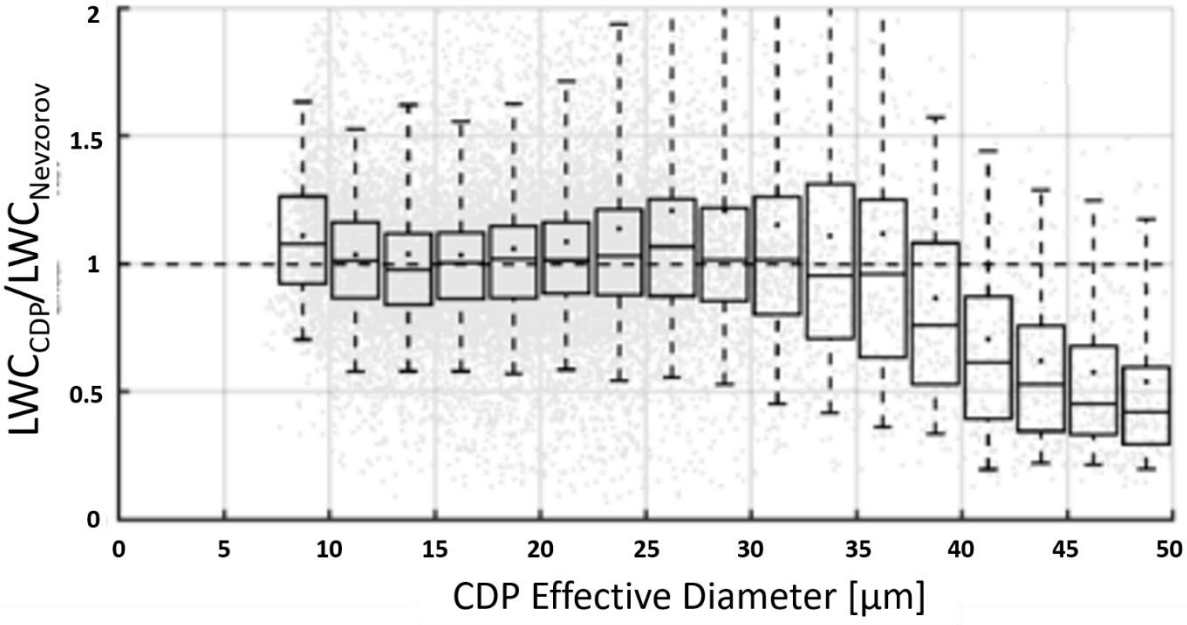

Figure S2 Ratio of total CDP LWC to corrected Nevzoroz LWC as a function of CDP effective diameter for each calibration method for CLARIFY flight C036. Grey crosses indicate individual 1 Hz data points. Black diamonds indicate median value of the LWC ratio, binned by effective diameter in 2.5 µm bins to serve as a trend line. Out of cloud data has been removed using a LWC threshold of 0.05 g m^3 for both probes.

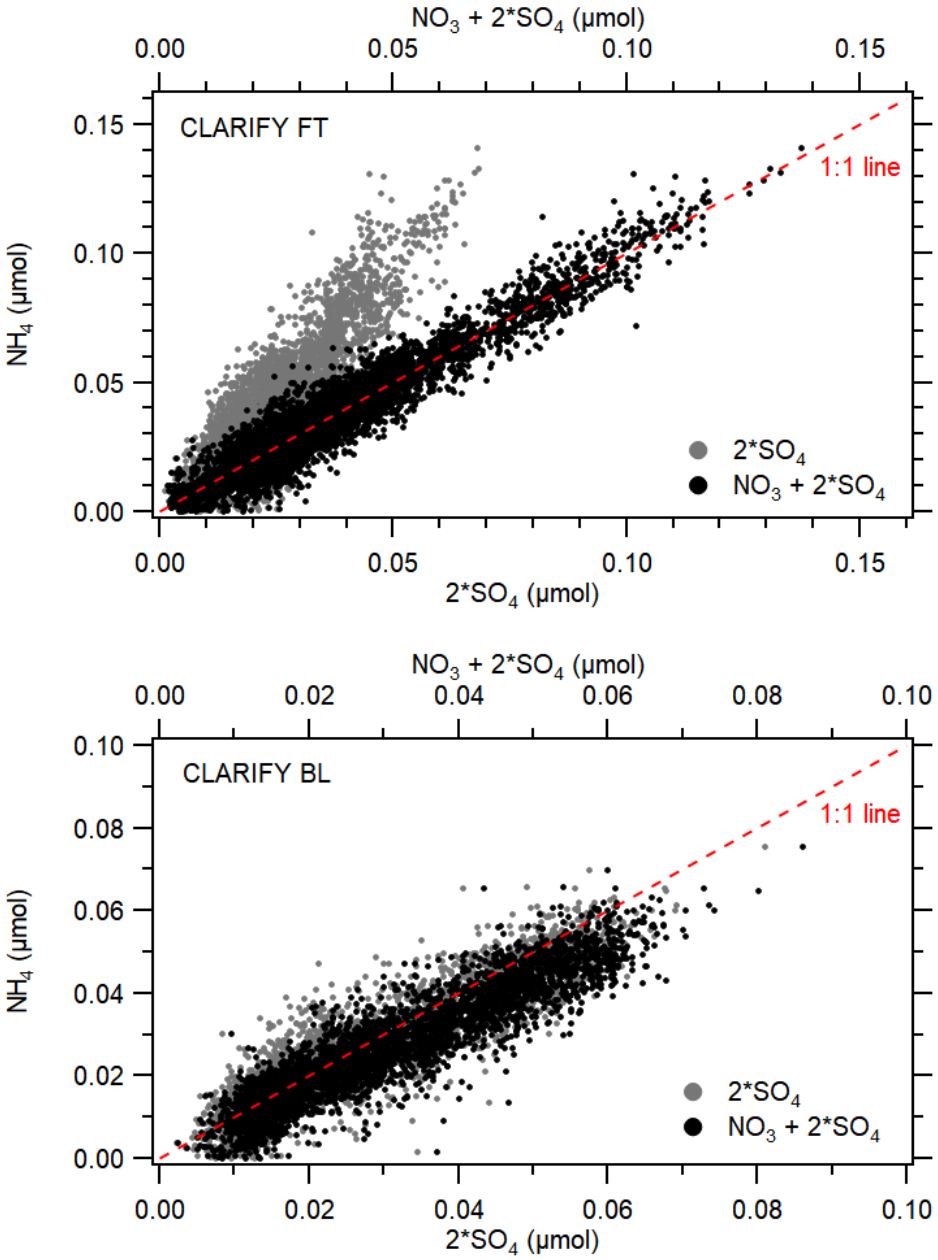

Figure S3 CLARIFY FAAM BAe-46 AMS data showing measured ammonium as a function of the molar sum of nitrate (NO_3) + 2* sulphate (SO_4) (black) and sulphate only (grey) for (a) the free troposphere and (b) boundary layer

205